first protonation step, making the proton less competitive. The difference is particularly evident between L1 and L3 where the introduction of a methyl group suppresses the protonic sponge behavior, making the basicity strength of L3 a few orders of magnitude smaller than that of L1. The consequence on the lithium complex stability is of the same order of magnitude (see Table VI). A similar trend is observed for L and its unmethylated derivative L4, where coupled to a reduced basicity of L with respect to L4 there is an enhancement of the lithium complex stability, which goes from log K = 4.8 for $[LiL4]^+$ up to log K = 5.5 for $[LiL]^+$ (see Table VI). The shortening of the hydrocarbon chains disposed around the apical group, which produces a smaller cage cavity, is the other important molecular parameter influencing the lithium complex stability: the $[LiL]^+$ complex is ca. 20 times more stable than $[LiL3]^+$ (see Table VI). That the Li^+ cation fits better into the smaller cavity of L, with respect to that present in L3, is also demonstrated by the X-ray analysis that has been carried out on $[LiL][BPh_4]$. In Figure 3, the ORTEP drawing of the $[LiL]^+$ complex cation is reported. The lithium atom is enclosed inside the cage cavity, adopting a fairly regular bipyramidal geometry with the Li-N distances in the 2.01-2.08 Å range. These distances, which are similar to those found for the unmethylated derivative $[LiL4]^+$,[6] are instead much shorter than those found in the Li^+ complexes either of the (211) cryptand (2.29 Å)[25] or of the related larger cage 5,12,17-trimethyl-1,5,9,12,17-pentaazabicyclo[7.5.5]nonadecane L3 (2.14-2.45 Å).[4]

Conclusions. The aim of this work was to synthesize an azacage with elevated binding capability toward Li^+ in aqueous solution. Previous experiences with other cages of the series have led to L, which is indeed the best lithium binder of the series. The high stability constant and the very regular coordination geometry, coupled with short Li-N bonds, are all good indications of an extremely good match between the cation radius and the cavity hole.

Acknowledgment. We thank the ISSECC (CNR) Institute of Florence for the use of a diffractometer. We also thank the Italian Minister of Scientific Research and the Italian Research National Council (CNR) for financial support.

Registry No. **1**, 90281-17-7; **2**·HCl, 55-86-7; $[H_3L][ClO_4]_3$, 135365-48-9; $[HL][BPh_4]$, 135365-49-0; $[LiL][ClO_4]$, 135393-35-0; $[LiL][BPh_4]$, 135501-17-6; $[CuL][ClO_4]_2$, 135393-37-2; $[HL][ClO_4]$, 135365-50-3.

Supplementary Material Available: Tables of complete positional and isotropic thermal parameters, hydrogen atom parameters, anisotropic thermal parameters, and bond lengths and angles (10 pages); listings of observed and calculated structure factors (21 pages). Ordering information is given on any current masthead page.

(25) Moras, D.; Weiss, R. *Acta Crystallogr.* **1973**, *B29*, 400.

Contribution from the Departments of Chemistry, Wayne State University, Detroit, Michigan 48202, and University of Wisconsin—Eau Claire, Eau Claire, Wisconsin 57401

Tetradentate Macrocyclic Complexes of Platinum. X-ray Crystal Structures and Redox Behavior of Complexes Containing Nitrogen or Sulfur Donor Atoms[1]

David Waknine,[2a] Mary Jane Heeg,[2a] John F. Endicott,*[,2a] and L. A. Ochrymowycz[2b]

Received February 14, 1991

Several complexes of platinum containing aliphatic tetradentate (N or S donors) macrocyclic (12-16-membered rings) ligands have been prepared and characterized. The most thoroughly examined of these complexes were those containing 14-membered macrocyclic ligands. In this series of complexes, the half-wave potential of the $Pt(MCL)^{2+}/Pt(MCL)Cl_2^{2+}$ couple (in 1 M NaCl) increased in a regular manner as secondary amine donors were successively replaced by thioether donors (MCL = a macrocyclic ligand). This pattern of behavior was correlated with changes of interligand repulsions (between axial Cl^- and the equatorially coordinated macrocycle) that accompany the change of ligand conformation from the axially unrestricted endo conformation of coordinated 1,4,7,11-tetraazacyclotetradecane ([14]aneN$_4$) to the somewhat restricted exo conformation adopted by 1,4,7,11-tetrathiacyclotetradecane ([14]aneS$_4$). Related shifts in potentials were found in methyl-substituted tetraazacyclotetradecane complexes. $[Pt([14]aneN_4)Cl_2]Cl_2{\cdot}HCl{\cdot}H_2O$, $PtN_4C_{10}H_{23}Cl_5O$, crystallizes in the monoclinic space group $P2_1/n$ with Z = 1 and a = 7.5059 (9) Å, b = 18.812 (5) Å, c = 7.669 (2) Å, and β = 99.09 (2)°. The structure refined to R = 0.050 and R_w = 0.062 for 1592 reflections. $[Pt(ms\text{-}(5,12)\text{-}Me_6[14]aneN_4)](ClO_4)_2{\cdot}2H_2O$, $PtN_4C_{16}H_{40}Cl_2O_{10}$ (*ms*-(5,12)-Me$_6$[14]aneN$_4$ = *meso*-5,7,7,12,14,14-hexamethyl-1,4,8,11-tetraazacyclotetradecane), crystallizes in the monoclinic space group $P2_1/c$ with Z = 2 and a = 10.0331 (9) Å, b = 16.198 (3) Å, c = 8.660 (1) Å, and β = 107.48 (1)°. The structure refined to R = 0.035 and R_w = 0.024 for 1526 reflections. $[Pt([14]aneS_4)](ClO_4)_2$, $PtS_4C_{10}H_{20}Cl_2O_8$, crystallizes in the monoclinic space group $P2_1/n$ with Z = 4 and a = 12.098 (1) Å, c = 12.557 (2) Å, and β = 98.69 (1)°. The structure refined to R = 0.043 and R_w = 0.042 for 2703 reflections.

Introduction

Transition-metal complexes with macrocyclic ligands have been useful in the study of metal oxidation-reduction behavior in well-defined coordination environments and often for generating metals in relatively rare oxidation states.[3-6] We have long had an interest in the chemical behavior of complexes with the relatively rare[7,8] low-spin d^7 electronic configuration.[9] While low-spin d^7 cobalt(II)[3-5,9b-d] and nickel(III)[4,5,9c,10-12] complexes can often be isolated and fully characterized, the rhodium(II)[9a] and platinum(III)[13] analogues are usually encountered as short-lived, transient species.

(1) (a) Partial support of the research at Wayne State University by the Division of Chemical Sciences, Office of Basic Energy Sciences, Office of Energy Research, U.S. Department of Energy, is gratefully acknowledged. (b) We are also grateful for partial support of the research at the University of Wisconsin—Eau Claire by the Research Corp. and by the donors of the Petroleum Research Fund, administered by the American Chemical Society.
(2) (a) Wayne State University. (b) University of Wisconsin—Eau Claire.
(3) Melson, G. A., Ed. *Coordination Chemistry of Macrocyclic Compounds*; Plenum: New York, 1979.
(4) Lindoy, L. F. *The Chemistry of Macrocyclic Ligand Complexes*; Cambridge University Press: Cambridge, U.K., 1989.
(5) Bernal, I., Ed. *Stereochemistry and Stereophysical Behavior of Macrocycles*; Elsevier: Amsterdam, 1987.
(6) Haines, R. I.; McAuley, A. *Coord. Chem. Rev.* **1981**, *39*, 77.
(7) Cotton, F. A.; Wilkinson, G. *Advanced Inorganic Chemistry*, 3rd ed.; Interscience: New York, 1972.
(8) Greenwood, N. N.; Earnshaw, A. *Chemistry of the Elements*; Pergamon: New York, 1984.
(9) (a) Lilie, J.; Simic, M. G.; Endicott, J. F. *Inorg. Chem.* **1975**, *14*, 2129. (b) Endicott, J. F.; Lilie, J.; Kuszaj, J. M.; Ramaswamy, B. S.; Schmonsees, W. G.; Simic, M. G.; Glick, M. D.; Rillema, D. P. *J. Am. Chem. Soc.* **1977**, *99*, 429. (c) Kumar, K.; Rotzinger, F. P.; Endicott, J. F. *J. Am. Chem. Soc.* **1983**, *105*, 7064. (d) Durham, B.; Anderson, T. J.; Switzer, J. A.; Endicott, J. F.; Glick, M. D. *Inorg. Chem.* **1977**, *16*, 271.
(10) Gore, E. S.; Busch, D. B. *Inorg. Chem.* **1973**, *12*, 1.
(11) Haines, R. I.; McAuley, A. *Coord. Chem. Rev.* **1981**, *89*, 77.
(12) Zeigerson, E.; Bar, I.; Bernstein, J.; Kirschenbaum, L. J.; Meyerstein, D. *Inorg. Chem.* **1982**, *21*, 73.
(13) (a) Waltz, W. L.; Lilie, J. *Inorg. Chem.* **1980**, *19*, 3284. (b) Storer, D. K.; Waltz, W. L. *Int. J. Radiat. Phys. Chem.* **1975**, *7*, 693.

0020-1669/91/1330-3691$02.50/0

The low-spin d^7 electronic configuration has been reported to be stabilized through the coordination of thioether ligands[14] to Co(II),[15,16] Rh(II),[17] Pd(III),[18] and Pt(III).[19] Most such complexes are coordinatively saturated so that access to a metal coordination site would be limited. Such access to the coordination sphere is important in many metal-mediated multielectron processes, metal-mediated radical reactions, etc. Of course, complexes in which the d^7 configuration is greatly stabilized would be unlikely to exhibit much interesting chemistry.

In principle, the lifetimes of metastable low-spin d^7 complexes might also be increased by stereochemical constraints imposed by coordinated macrocyclic ligands.[3-5] For example, the macrobicyclic "sepulchrate" (sep)[20] ligand so favors 6-coordination that it inhibits the formation of a 4-coordinate Pt(II) product on reduction of $Pt(sep)^{4+}$.[21] This example illustrates one way in which transition-metal-bonding requirements and the constraints imposed by ligand stereochemistry can combine to block normal redox pathways. Similarly, the changes of coordination, from octahedral (low spin d^6) through tetragonally distorted (low spin d^7) to square planar (low spin d^8) that accompany successive reductions of Pt(IV) suggest that it might be possible to design complexes in which the low-spin d^7 configuration is kinetically stabilized without blocking the axial access (to the metal), which seems so important in much platinum chemistry. There have previously been several reports of palladium[22,23] and of platinum[22-29] complexes with macrocyclic ligands. In this report, we describe the synthesis and characterization of a series of platinum complexes whose macrocyclic ligands span a range of small stereochemical perturbations. Some preliminary investigations of the redox behavior of these complexes indicate that ligand stereochemistry does play a very important role.

Experimental Section

Materials. Tetraazamacrocyclic ligands were available from previous studies in this laboratory.[30] The cyclic thioether ligands have been reported in studies from Professor D. B. Rorabacher's laboratory,[31] and their synthesis is reported elsewhere.

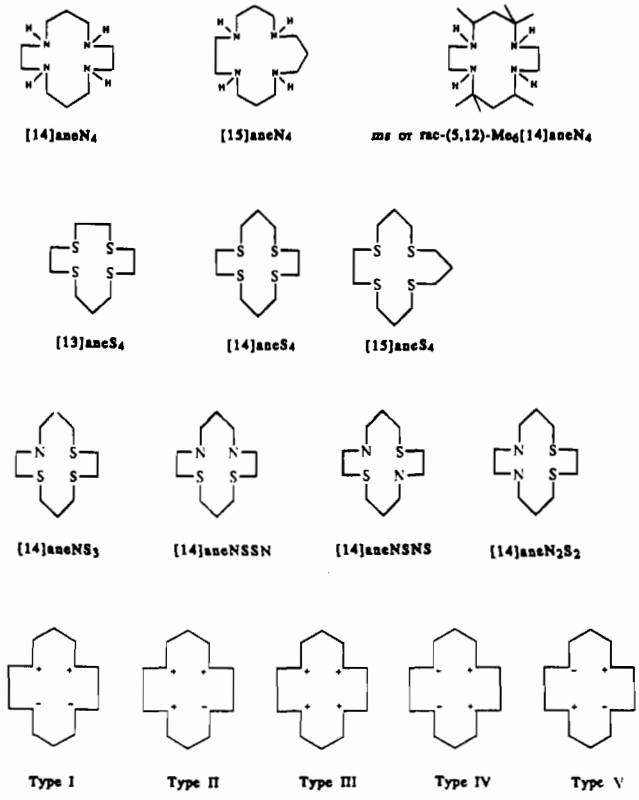

Figure 1. Structures of the ligands.

[Pt(*ms*-(5,12)-Me_6[14]aneN$_4$)]Cl_2. Approximately 0.6 mmol of K_2PtCl_4 was dissolved with stirring in about 10 mL of DMSO. The clear yellow solution was stirred for an additional 20 min under a nitrogen atmosphere. Approximately 0.66 mmol of the ligand, *ms*-(5,12)-Me_6[14]aneN$_4$·2H_2O (see Figure 1), was dissolved in 10 mL of DMSO in a three-neck round-bottom flask, and the solution was purged with a stream of N_2. The platinum solution was added dropwise over about 10 min to the solution of the ligand maintained at about 65 °C. The yellow color faded over about a 1-h period, and a white precipitate was obtained when this solution was cooled to room temperature and mixed with about 10 mL of diethyl ether. This precipitate was removed by filtration and washed with two 1-mL portions of cold ethanol. The resulting white solid was dissolved in 5 mL of H_2O and the solution passed through a fine-frit funnel. This colorless solution was rotatory-evaporated to about half the volume and cooled to give colorless crystals. Metathesis to PF_6^-, ClO_4^-, and $CF_3SO_3^-$ salts was accomplished by dissolving [Pt(*ms*-(5,12)-Me_6[14]aneN$_4$)]Cl_2 in a minimum amount of water and adding an excess of the desired salt.

Warning! The perchlorate salts prepared in this work are potentially explosive and must be handled with great care.

[Pt(*rac*-(5,12)-Me_6[14]aneN$_4$)]Cl_2 and **[Pt(*N*-Me_4[14]aneN$_4$)]Cl_2**[20] were prepared by using the above procedure except that dry acetone was added to the reaction mixture to precipitate the products.

[Pt([14]aneN$_4$)]Cl_2. Oxygen had to be more rigorously excluded from this synthesis than from those described above. Similar procedures were used, precipitating the product with acetone and washing it with chloroform. We also prepared this complex using a variation of the above procedure in which the ligand was dissolved in a (1:1, v/v) mixture of CH_3CN and CH_3NO_2 at 50 °C and the resulting solution was mixed with K_2PtCl_4 in DMSO and refluxed for 10 min.

[Pt([14]aneN$_4$)Cl_2]Cl_2·HCl·H_2O. This complex was prepared by dissolving [Pt([14]aneN$_4$)]Cl_2 in aerated aqueous HCl (~0.1 M) and allowing the solvent to evaporate.

[Pt([15]aneN$_4$)]Cl_2. Approximately 0.25 mmol of K_2PtCl_4 and 0.28 mmol of [15]aneN$_4$ were introduced into a 50-mL round-bottom flask

(14) Cooper, S. C.; Rawle, S. C. *Struct. Bonding (Berlin)* **1990**, *72*, 1.
(15) Setzer, W. N.; Ogle, C. A.; Wilson, G. S.; Glass, R. S. *Inorg. Chem.* **1983**, *22*, 266.
(16) Hartman, J. R.; Hintsa, E. J.; Cooper, S. R. *J. Am. Chem. Soc.* **1986**, *108*, 1208.
(17) Rawle, S. C.; Yagbasan, R.; Prout, K.; Cooper, S. R. *J. Am. Chem. Soc.* **1987**, *109*, 6181.
(18) Blake, A. J.; Holder, A. J.; Hyde, T. I.; Schröder, M. *J. Chem. Soc., Chem. Commun.* **1987**, 987.
(19) Blake, A. J.; Gould, R. O.; Holder, A. J.; Hyde, T. I.; Lavery, A. J.; Odulate, M. O.; Schröder, M. *J. Chem. Soc., Chem. Commun.* **1987**, 118.
(20) Abbreviations: pn = 1,3-propylenediamine; en = 1,2-ethylenediamine; [14]aneN$_4$ = cyclam = 1,4,8,11-tetraazacyclotetradecane; *ms*-(5,12)-Me_6[14]aneN$_4$ = *meso*-5,7,7,12,14,14-hexamethyl-1,4,8,11-tetraazacyclotetradecane; dioxocyclam = 5,7-dioxo-1,4,8,11-tetraazacyclotetradecane; dbtaa = dibenzo-1,4,8,11-tetraaza[14]annulene; $(NHOH)_2$sar = 1,8-bis(hydroxylamino)-3,6,10,13,16,19-hexaazabicyclo[6.6.6]icosane; *rac*-(5,12)-Me_6[14]aneN$_4$ = *rac*-5,7,7,12,14,14-hexamethyl-1,4,8,11-tetraazacyclotetradecane; Me_4[14]aneN$_4$ = 1,4,8,11-tetramethyl-1,4,8,11-tetraazacyclotetradecane; [15]aneN$_4$ = 1,4,8,12-tetraazacyclopentadecane; [12]aneS$_4$ = 1,4,7,10-tetrathiacycloduodecane; [14]aneS$_4$ = 1,4,8,11-tetrathiacyclotetradecane; [15]aneN$_4$ = 1,4,8,12-tetrathiacyclopentadecane; [16]aneS$_4$ = 1,5,9,13-tetrathiacyclohexadecane; [14]aneNS$_3$ = 1-aza-4,8,11-trithiacyclotetradecane; [14]aneN$_2$S$_2$ = 1,4-diaza-8,11-dithiacyclotetradecane; [14]aneNSNS = 1,8-diaza-4,11-dithiacyclotetradecane; [14]aneNSSN = 1,11-diaza-4,8-dithiacyclotetradecane.
(21) Boucher, H. A.; Lawrance, G. A.; Lay, P. A.; Sargeson, A. M.; Bond, A. M.; Sangster, D. F.; Sullivan, J. C. *J. Am. Chem. Soc.* **1983**, *105*, 4652.
(22) Schröder, M. *Pure Appl. Chem.* **1988**, *80*, 517.
(23) Toriumi, K.; Yamashita, M.; Ito, H.; Ito, T. *Acta Crystallogr.* **1986**, *C42*, 963.
(24) Kimura, E.; Korenari, S.; Shionoya, M.; Shiro, M. *J. Chem. Soc., Chem. Commun.* **1988**, 1166.
(25) McCrindle, R.; Ferguson, G.; McAlees, A. J.; Parvez, M.; Ruhl, B. L.; Stephenson, D. K.; Wieckowski, T. *J. Chem. Soc., Dalton Trans.* **1986**, 2351.
(26) Jircitano, A. J.; Timken, M. D.; Mertes, K. B.; Ferraro, J. R. *J. Am. Chem. Soc.* **1979**, *101*, 7661.
(27) Blake, A. J.; Gould, R. O.; Lavery, A. J.; Schroder, M. *Angew. Chem., Int. Ed. Engl.* **1986**, *25*, 274.
(28) Kyba, E. P.; Davis, R. E.; Fox, M. A.; Clubb, C. N.; Liu, S.-T.; Reitz, G. A.; Schleuler, V. J.; Kashyap, R. P. *Inorg. Chem.* **1987**, *26*, 1647.
(29) Hunziker, M.; Rihs, G. *Inorg. Chim. Acta* **1985**, *102*, 39.
(30) (a) Lessard, R. B.; Endicott, J. F.; Perkovic, M. W.; Ochrymowycz, L. A. *Inorg. Chem.* **1989**, *28*, 2574. (b) Lessard, R. B.; Heeg, M. J.; Buranda, T. J.; Perkovic, M. W.; Schwarz, C. L.; Endicott, J. F. *Inorg. Chem.*, submitted for publication.
(31) Pett, V. B.; Diaddario, L. L.; Dockal, E. R.; Corfield, P. W.; Ceccarelli, C.; Glick, M. D.; Ochrymowycz, L. A.; Rorabacher, D. B. *Inorg. Chem.* **1983**, *22*, 3661.

Table I. Elemental Analyses

complex	% found (calcd) C	H	N	other
$[Pt([14]aneN_4)](PF_6)_2$	17.52	3.53	8.17	9.04 (P)
	(17.45)	(3.49)	(8.13)	(9.04)
$[Pt(ms\text{-}(5,12)\text{-}Me_6[14]aneN_4)](CF_3SO_3)_2$	27.80	4.66	7.20	
	(27.19)	(4.69)	(7.35)	
$[Pt(ms\text{-}(5,12)\text{-}Me_6[14]aneN_4)][Pt(CN)_4]$	30.86	4.68	14.63	
	(30.84)	(4.66)	(14.39)	
$[Pt(rac\text{-}(5,12)\text{-}Me_6[14]aneN_4)](ClO_4)_2$	28.32	5.35	8.26	10.45 (Cl)
	(28.41)	(5.80)	(7.88)	(10.40)
$[Pt([14]ane(NCH_3)_4)](PF_6)_2$	22.68	4.35	7.56	8.35 (P)
	(22.47)	(4.25)	(7.46)	(8.40)
$[Pt([14]aneS_4)](ClO_4)_2$	17.65	3.26		
	(17.55)	(3.28)		
$[Pt([15]aneS_4)](PF_6)_2$	17.21	2.89		16.71 (S)
	(17.32)	(2.84)		(16.47)

that was flushed with a stream of purified N_2. A 7-mL aliquot of DMSO was deaerated and then added to these solids under N_2; the temperature of the mixture was raised to 102 °C for about 30 min. The temperature of this pale yellow solution was increased quickly to 115 °C for 3 min; then the solution was cooled. Excess acetone was added to the solution at room temperature to produce a white precipitate.

$[Pt([14]aneS_4)]Cl_2$. Approximately 0.25 mmol of K_2PtCl_4 was dissolved in 45 mL of DMSO, CH_3CN, and CH_3NO_2 (2:1:1, v/v/v), and the solution was deaerated. After 5 min, the solution was added to a solution formed from 0.275 mmol of the ligand in the same mixture of solvents. A pink particulate suspension formed on mixing. The suspension became white when the mixture was boiled. When the solution that resulted from 2 min of refluxing was cooled to room temperature, a white crystalline solid formed. This was removed by filtration and washed with ether. Additional product was obtained by adding the original filtrate to a larger volume of acetone.

$[Pt([13]aneS_4)]Cl_2$. The product, obtained by procedures analogous to the preceding, was pale yellow. **$[Pt(L)]Cl_2$** complexes with L = [14]aneNS$_3$, [14]aneN$_2$S$_2$, [14]aneNSSN, and [14]aneNSNS were obtained by using minor variations of the procedures described above.

Techniques. Complexes were characterized by elemental analysis, electrochemical behavior, spectroscopic properties, and X-ray crystallography. Elemental analyses were obtained from Midwest Microanalytical Laboratories. Cyclic voltammetric determinations were performed by using a BAS-10 instrument with a platinum working electrode and Ag/AgCl reference. Infrared spectra were obtained on a Nicolet 20DX-FT IR spectrometer, and ^1H NMR spectra were obtained on a Nicolet QE-300 instrument.

Crystallography. All single-crystal X-ray diffraction experiments were performed on a Nicolet R3 automated diffractometer with Mo Kα radiation (λ = 0.710 73 Å) and a graphite monochromator at ambient temperature.

$[Pt([14]aneN_4)Cl_2]Cl_2\cdot HCl\cdot H_2O$. Details of the data collection were as follows: scan method, $\theta/2\theta$; scan range, 1.0° below Kα_1 to 1.1° above Kα_2; scan rate, variable, 2–5°/min; ratio of background to scan time, 0.5. The structure was solved by Patterson methods and refined in a full matrix with the programs of SHELX-76.[32] All non-hydrogen atoms were refined anisotropically. Hydrogen atoms were placed in calculated positions and held invariant. No hydrogen atoms were placed on solvent molecules. No correction for secondary extinction was made. Neutral-atom scattering factors and corrections for anomalous dispersion were from ref 33. Abbreviated crystallographic data for $[Pt([14]aneN_4)Cl_2]Cl_2\cdot HCl\cdot H_2O$ follow: formula $PtN_4C_{10}H_{23}Cl_5O$, fw 587.68, colorless rod-shaped crystals, 0.26 × 0.22 × 0.62 mm^3, monoclinic crystal system, space group $P2_1/n$, a = 7.5059 (9) Å, b = 18.812 (5) Å, c = 7.669 (2) Å, β = 99.09 (2)°, V = 1069.3 (4) Å^3, Z = 2, F_{000} = 564 e, density(calc) = 1.825 g cm^{-3}, 2θ range 6–50°, hkl (ranges $-9 \le h \le 9$, $0 \le k \le 23$, $-10 \le l \le 10$, 4028 total data collected, 1592 observed unique data with $I \ge 3\sigma(I)$, μ = 72.64 cm^{-1}, absorption corrections by empirical methods[34] yielding transmission coefficients 0.251–0.141, final conventional R value 0.050, final weighted R value 0.062, weight $(\sigma_F)^{-2}$. Lattice constants were derived from 25 high-angle ($2\theta > 20°$) reflections constrained monoclinic.

$[Pt(ms\text{-}(5,12)\text{-}Me_6[14]aneN_4)](ClO_4)_2\cdot 2H_2O$. The sample crystal was sealed in a thin-walled capillary to prevent decomposition due to solvent loss. Details of the data collection were as follows: scan method, $\theta/2\theta$; scan range, 0.9° below Kα_1 to 1.2° above Kα_2; scan rate, variable, 2–10°/min; ratio of background to scan time, 0.5. The structure was solved by Patterson methods and refined in a full matrix with the programs of SHELX-76.[32] All non-hydrogen atoms were refined anisotropically. Hydrogen atoms were placed in observed or calculated positions and held invariant. Four reflections were removed due to secondary extinction. Neutral-atom scattering factors and corrections for anomalous dispersion were from ref 33. Abbreviated crystallographic data for $[Pt(ms\text{-}(5,12)\text{-}Me_6[14]aneN_4)](ClO_4)_2\cdot 2H_2O$ follow: formula $PtN_4C_{16}H_{40}Cl_2O_{10}$, fw 714.51, colorless rod-shaped crystals, 0.34 × 0.22 × 0.24 mm,[34] monoclinic crystal system, space group $P2_1/c$, a = 10.0331 (9) Å, b = 16.198 (3) Å, c = 8.660 (1) Å, β = 107.48 (1)°, V = 1342.4 (3) Å^3, Z = 2, F_{000} = 712 e, d(calc) = 1.768 g cm^{-3}, 2θ range 5–50°, hkl ranges $0 \le h \le 12$, $0 \le k \le 20$, $-11 \le l \le 11$, 3086 total data collected, 1526 observed unique data with $I \ge 2.5\sigma(I)$, μ = 55.31 cm^{-1}, absorption corrections by empirical methods[33] yielding transmission coefficients 0.299–0.241, final conventional R value 0.035, final weighted R value 0.024, weight $(\sigma_F)^{-2}$. Lattice constants were derived from 25 high-angle ($2\theta > 20°$) reflections constrained monoclinic.

$[Pt([14]aneS_4)](ClO_4)_2$. Details of the data collection were as follows: scan method, $\theta/2\theta$; scan range, 1.0° below Kα_1 to 1.0° above Kα_2; scan rate, variable, 2–5°/min; ratio of background to scan time, 0.5. The structure was solved by Patterson methods and refined in a full matrix with the programs of SHELX-76.[31] All non-hydrogen atoms were refined anisotropically. Hydrogen atoms were placed in calculated positions and held invariant. A systematic correction[32] for secondary extinction was made so that $F_{cor} = F(1 - 10^{-4}F^2/\sin\theta)$ where x refined to 0.002 52. Neutral-atom scattering factors and corrections for anomalous dispersion were from ref 33. Abbreviated crystallographic data for $[Pt([14]aneS_4)](ClO_4)_2$ follow: formula $PtS_4C_{10}H_{20}Cl_2O_8$, fw 662.52, colorless multifaceted crystals, 0.40 × 0.30 × 0.20 mm^3, monoclinic crystal system, space group $P2_1/n$, a = 12.098 (1) Å, b = 12.650 (3) Å, c = 12.557 (2) Å, β = 98.69 (1)°, V = 1899.6 (5) Å^3, Z = 4, F_{000} = 1280 e, d(calc) = 2.316 g cm^{-3}, 2θ range 6–52°, hkl ranges $0 \le h \le 15$, $0 \le k \le 16$, $-16 \le l \le 16$, 4228 total data collected, 2703 observed unique data with $I \ge 3\sigma(I)$, μ = 82.04 cm^{-1}, absorption corrections by empirical methods[34] yielding transmission coefficients 0.224–0.105, final conventional R value 0.043, final weighted R value 0.042, weight $(\sigma_F)^{-2}$. Lattice constants were derived from 25 high-angle ($2\theta > 20°$) reflections constrained monoclinic.

Results

The compounds synthesized have been characterized by elemental analysis, electrochemistry, ^1H NMR spectroscopy, and X-ray crystallography. The quantities of ligand available were very small in some instances, thus limiting the number of characterizations possible. Elemental analyses are summarized in Table I. ^1H NMR spectra of the simpler complexes are shown in Figures 2 and 3.

Electrochemical oxidations of the Pt(II) complexes were irreversible in perchlorate or in trifluoromethanesulfonate media but they were generally quasi-reversible in 1 M NaCl (Figure 4). In general, the half-wave potential became smaller in proportion to [Cl$^-$]. In weakly complexing media, the anodic peaks were usually very broad and there was little evidence for cathodic peaks. In

(32) Sheldrick, G. M. SHELX-76. University Chemical Laboratory, Cambridge, England, 1976.
(33) *International Tables for X-ray Crystallography*; Kynoch Press: Birmingham, England, 1974; Vol. 4.
(34) Sheldrick, G. M. SHELXTL. University of Gottingen, Federal Republic of Germany, 1978.

Table II. Cyclic Voltammetric Parameters for Oxidations of Several $Pt(MCL)^{2+}$ Complexes

MCL	medium	scan rate, mV/s	$E_{1/2}$,[a] V	ΔE_p, mV
[14]aneN$_4$	1 M NaCl(aq)	250	0.384	184
		50	0.382	284
		20	0.390	161
[15]aneN$_4$	1 M NaCl(aq)	100	0.399	396
		50	0.402	209
ms-(5,12)-Me$_6$[14]aneN$_4$	1 M NaCl(aq)	500	0.597 ± 0.014	152 ● 51
		400	0.604	
		300	0.626 ± 0.002	215 ± 40
		200	0.597	140
		100	0.598 ± 0.001	90 ± 25
		50	0.594	122
		10	0.590 ± 0.001	65 ± 20
		2	0.588	48
		1	0.589	64
	1 M NaCl + 0.5 M NaClO$_4$(aq)	50	0.600	48
	1 M NaCl + 0.5 M Na$_2$SO$_4$(aq)	150	0.590	61
rac-(5,12)-Me$_6$[14]aneN$_4$	1 M NaCl(aq)	100	0.63	71
[14]aneNSNS	1 M NaCl(aq)	100	irrev	
[14]aneNSSN	1 M NaCl(aq)	100	0.55 (irrev)[b]	
			0.65 (irrev)[b]	
[14]aneN$_2$S$_2$	1 M NaCl(aq)	100	0.73	196
[14]aneS$_4$	1 M NaCl(aq)	200	0.835	92
		100	0.837 ± 0.004	111 ± 40
		50	0.842	113
	01. M NaCl + 0.5 M NaClO$_4$(aq)	10	0.938	71
		5	0.942	147
[14]aneS$_4$	0.1 M TEAP–CH$_3$CN	20	~0.7 (irrev)[b]	
			~1.0 (irrev)[b]	
[15]aneS$_4$	1 M NaCl(aq)	100	0.735 ± 0.005	96 ● 20
[16]aneS$_4$	1 M NaCl(aq)	100	0.68	51

[a] Vs Ag/AgCl. Average values and standard deviations for three or more separate determinations; otherwise, a single solution was used. [b] Anodic peak; the cathodic peak was very small.

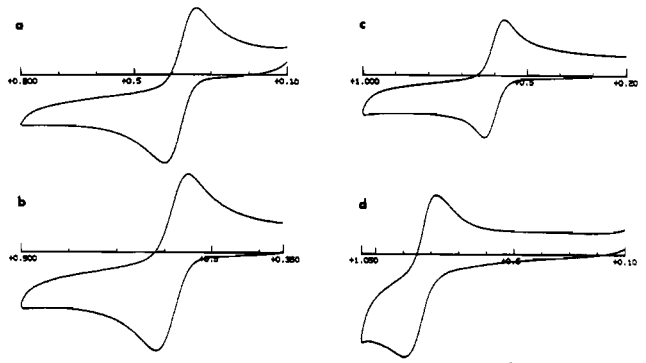

Figure 2. Cyclic voltammograms: (a) $Pt([14]aneN_4)^{2+}$; (b) $Pt(ms\text{-}(5,12)\text{-}Me_6[14]aneN_4)^{2+}$; (c) $Pt(rac\text{-}(5,12)\text{-}Me_6[14]aneN_4)^{2+}$; (d) $Pt([14]aneS_4)^{2+}$. All measurements are vs Ag/AgCl in 1 M aqueous NaCl at 100 mV s^{-1} scan rates (except for scan b, with a 150 mV s^{-1} scan rate).

two instances, for $Pt([14]aneS_4)^{2+}$ in CH_3CN and for $Pt([14]aneNSSN)^{2+}$ in aqueous NaCl, we observed two anodic peaks coupled to poorly defined (in the former) or no (in the latter) cathodic peaks. The separation of cathodic and anodic peaks, ΔE_p, was found to be scan rate dependent for $Pt(ms\text{-}(5,12)\text{-}Me_6[14]aneN_4)^{2+}$ (in aqueous NaCl), and it became appreciably more reversible at very small scan rates. The half-wave potentials ($E_{1/2} = (E_a + E_c)/2$) of the $Pt(MCL)^{2+}$ complexes were strongly dependent on the macrocyclic ligand. The electrochemical results are summarized in Table II.

Crystallographic Results. *trans*-[Pt([14]aneN$_4$)Cl$_2$]Cl$_2$·HCl·H$_2$O. Fractional atomic coordinates and bond lengths and angles are given in Tables III and IV. The geometry and labeling are shown in Figure 5. The Pt complex is octahedrally 6-coordinate and exists as discrete neutral molecules. Intermolecular contacts, which might indicate hydrogen bonding, are present between the amine hydrogen atom and coordinated Cl (HN1···Cl1′ = 2.564 Å), between the amine hydrogen atom and Cl$^-$ anion (HN2···Cl2 = 2.177 Å), and between the solvated H$_2$O, Cl$^-$, and HCl (O1···Cl2 = 3.357 Å, O1···Cl3 = 3.074 Å). The oxygen atom and chloride ion in the solvates occupy crystallographic mirror planes in the cell. The Pt atom occupies a crystallographic inversion center. Pt and the four nitrogen donor atoms are required to be planar. The Pt–Cl bond vector makes an angle of 87 (1)° with the equatorial plane. The five-membered rings are gauche δλ, and the six-membered rings are in chair conformations. The configuration at the N atoms is meso-*RSSR*, which corresponds to a type III configuration (lone pairs down–down–up–up) by Curtis[35]

Table III. Fractional Atomic Positional Parameters for [Pt([14]aneN$_4$)Cl$_2$]Cl$_2$·HCl·H$_2$O

atom	*x*	*y*	*z*
Pt1	1.00000	0.50000	0.00000
Cl1	0.8104 (5)	0.5540 (2)	0.1692 (5)
N1	0.788 (2)	0.4615 (7)	−0.175 (2)
N2	0.972 (2)	0.4081 (7)	0.134 (2)
C1	0.705 (2)	0.4025 (9)	−0.088 (2)
C2	0.857 (2)	0.3587 (9)	0.008 (2)
C3	1.144 (2)	0.3736 (9)	0.224 (2)
C4	1.260 (2)	0.424 (1)	0.342 (2)
C5	1.348 (2)	0.4854 (9)	0.247 (2)
Cl2	0.7692 (6)	0.3838 (3)	0.4600 (6)
Cl3	0.458 (1)	0.25000	0.027 (1)
O1	0.530 (3)	0.75000	−0.430 (3)

Table IV. Bond Lengths (Å) and Angles (deg) for $Pt([14]aneN_4)Cl_2^{2+}$

Pt1–Cl1	2.307 (4)	N2–C2	1.51 (2)
Pt1–N1	2.048 (13)	N2–C3	1.51 (2)
Pt1–N2	2.039 (13)	C1–C2	1.51 (2)
N1–C1	1.48 (2)	C3–C4	1.50 (3)
N1–C5′	1.47 (2)	C4–C5	1.56 (2)
Pt–N1–C1	107.8 (9)	N1–C1–C2	107 (1)
Pt1–N1–C5′	115 (1)	N1–C5′–C4′	111 (1)
Pt1–N2–C2	107.0 (8)	N2–C2–C1	107 (1)
Pt1–N2–C3	117 (1)	N2–C3–C4	112 (1)
Cl1–Pt1–N1	92.3 (4)	C1–N1–C5′	111 (1)
Cl1–Pt1–N2	88.1 (4)	C2–N2–C3	113 (1)
N1–Pt1–N2	84.3 (5)	C3–C4–C5	116 (1)

(35) Curtis, N. F. In *Coordination Chemistry of Macrocyclic Compounds*; Melson, G. A., Ed.; Plenum: New York, 1979; Chapter 4.

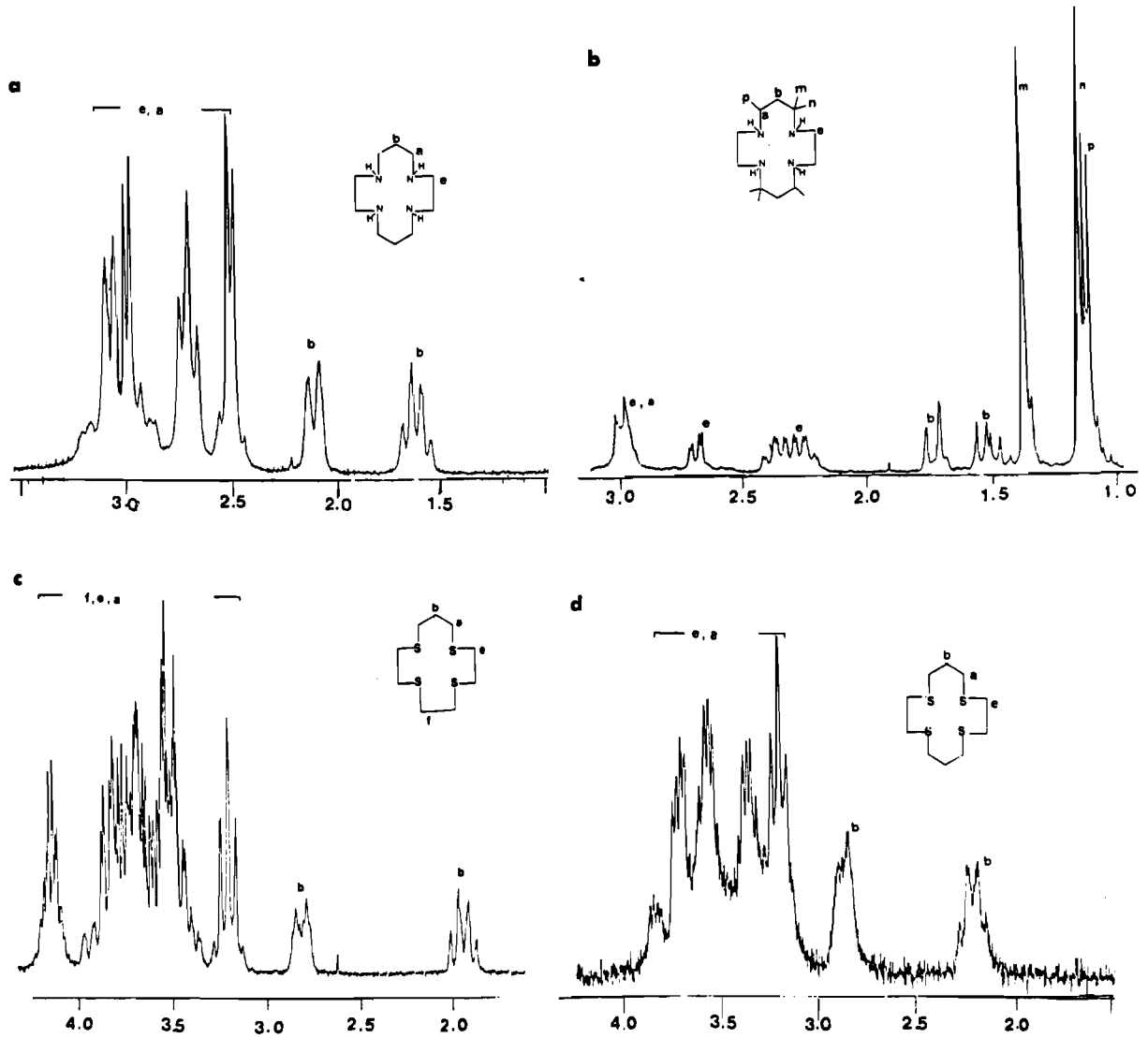

Figure 3. ^{1}H NMR spectra: (a) Pt([14]aneN$_4$)$^{2+}$; (b) Pt(*ms*-(5,12)-Me$_6$[14]aneN$_4$)$^{2+}$; (c) Pt([13]aneS$_4$)$^{2+}$; (d) Pt([14]aneS$_4$)$^{2+}$. Methylene peaks next to the donor atoms of the various chelate rings (designated a, e, f) have not been specifically assigned. D_2O solvent was used in all cases. Horizontal scales are in ppm vs TMS.

Table V. Fractional Atomic Positional Parameters for [Pt(*ms*-(5,12)-Me$_6$[14]aneN$_4$)](ClO$_4$)$_2$·2H$_2$O

atom	*x*	*y*	*z*
Pt1	0.00000	0.00000	0.00000
N1	0.1690 (8)	0.0767 (5)	0.0480 (9)
N2	0.1136 (8)	−0.1067 (5)	0.0125 (9)
C1	0.301 (1)	0.0476 (8)	0.168 (1)
C2	0.427 (1)	0.1097 (8)	0.187 (1)
C3	0.343 (1)	−0.0385 (8)	0.118 (2)
C4	0.253 (1)	−0.1124 (6)	0.140 (1)
C5	0.331 (1)	−0.1919 (7)	0.110 (1)
C6	0.241 (1)	−0.1158 (7)	0.314 (1)
C7	0.023 (1)	−0.1797 (6)	0.021 (2)
C8	−0.125 (1)	−0.1595 (7)	−0.097 (1)
Cl1	0.2342(3)	0.3934 (2)	0.1286 (4)
O1	0.218 (3)	0.3512 (9)	0.247 (2)
O2	0.318 (1)	0.3456 (7)	0.065 (1)
O3	2.295 (1)	0.4645 (6)	0.192 (2)
O4	0.128 (1)	0.409 (1)	0.024 (2)
O5	0.1417 (8)	−0.1187 (6)	0.6892 (9)

after Bosnich.[36] Bite angles here are normal at 84.3 (5)° for en and 95.7 (5)° for pn. A side view showing the conformation of the macrocycle is given in Figure 6. The Pt–N bond length averages 2.04 (1) Å and Pt–Cl = 2.307 (4) Å.

(36) Bosnich, B.; Poon, C. K.; Tobe, M. L. *Inorg. Chem.* **1985**, *4*, 1102.

Table VI. Bond Lengths (Å) and Angles (deg) for [Pt(*ms*-(5,12)-Me$_6$[14]aneN$_4$)](ClO$_4$)$_2$·2H$_2$O

Pt1–N1	2.042 (8)	C3–C4	1.54 (2)
Pt1–N2	2.056 (8)	C4–C5	1.57 (2)
N1–C1	1.49 (1)	C4–C6	1.55 (1)
N1–C8′	1.52 (1)	C7–C8	1.56 (2)
N2–C4	1.50 (1)	Cl1–O1	1.28 (1)
N2–C7	1.51 (1)	Cl1–O2	1.37 (1)
C1–C2	1.59 (2)	Cl1–O3	1.34 (1)
C1–C3	1.55 (2)	Cl1–O4	1.20 (1)
Pt1–N1–C1	117.4 (6)	C1–C3–C4	116.8 (9)
Pt1–N1–C8′	107.4 (6)	C2–C1–C3	109.1 (8)
Pt1–N2–C4	118.0 (6)	C3–C4–C5	106.4 (8)
Pt1–N2–C7	109.1 (6)	C3–C4–C6	111.5 (8)
N1–Pt1–N2	95.0 (3)	C4–N2–C7	111.0 (8)
N1–C1–C2	112.8 (9)	C5–C4–C6	108.9 (8)
N1–C1–C3	110.4 (8)	O1–C11–O2	105.1 (9)
N1–C8′–C7′	107.5 (8)	O1–C11–O3	106.4 (9)
N2–C4–C3	108.1 (8)	O1–C11–O4	114 (1)
N2–C4–C5	109.0 (7)	O2–C11–O3	112.9 (7)
N2–C4–C6	112.8 (8)	O2–C11–O4	109.4 (9)
N2–C7–C8	105.7 (8)	O3–C11–O4	109 (1)
C1–N1–C8′	111.0 (7)		

[Pt(*ms*-(5,12)-Me$_6$[14]aneN$_4$)](ClO$_4$)$_2$·2H$_2$O. Final fractional coordinates are given in Table V. The molecular geometry and labeling are shown in Figure 7. Bond lengths and angles are listed in Table VI. The Pt ion is in a square-planar environment within

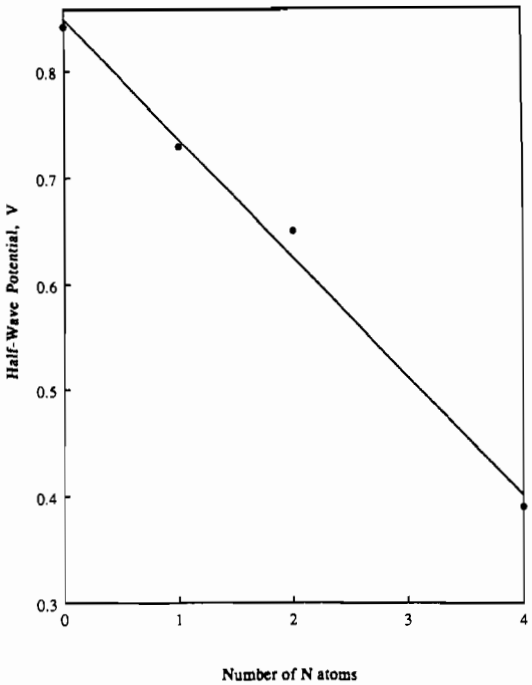

Figure 4. Variation of $E_{1/2}$ for $Pt([14]aneN_4S_b)^{2+}$ complexes with the increase in N donor atoms. Measurements are vs Ag/AgCl in 1 M aqueous NaCl.

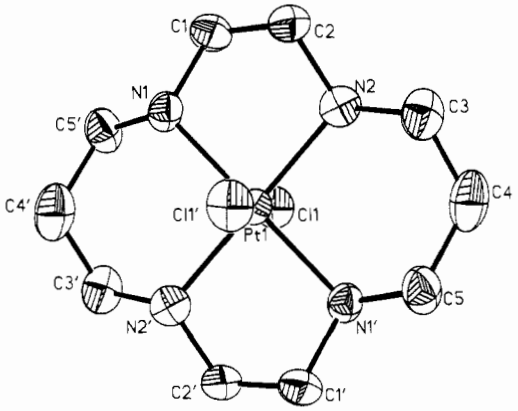

Figure 5. Perspective view of *trans*-$Pt([14]aneN_4)Cl_2^{2+}$ showing the labeling and geometry. All thermal ellipsoids in this and the other figures represent 50% probability. The Pt atom occupies a crystallographic inversion center.

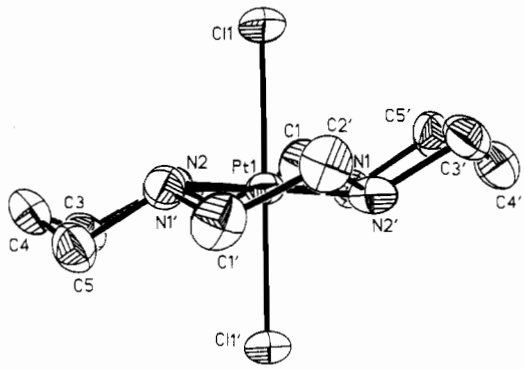

Figure 6. Side view of the macrocyclic in *trans*-$Pt([14]aneN_4)Cl_2^{2+}$ showing the labeling and geometry. The Pt atom occupies a crystallographic inversion center.

the macrocycle. The shortest intermolecular contact to Pt involves the hydrate: Pt···O5 = 3.906 Å. Hydrogen bonds to the amine protons are evident (O1···HN1 = 2.237 Å and O5···HN2 = 2.138 Å) as are hydrogen bonds to the solvated water (O3···HO5A = 2.689 Å and O4···HO5B = 1.856 Å). The cation occupies a

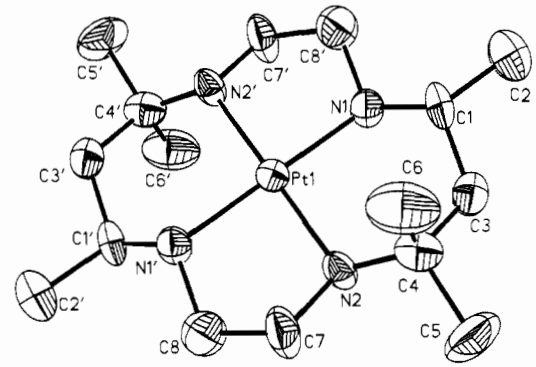

Figure 7. Perspective view of $Pt(ms\text{-}(5,12)\text{-}Me_6[14]aneN_4)^{2+}$ showing the labeling and geometry. The Pt atom occupies a crystallographic inversion center.

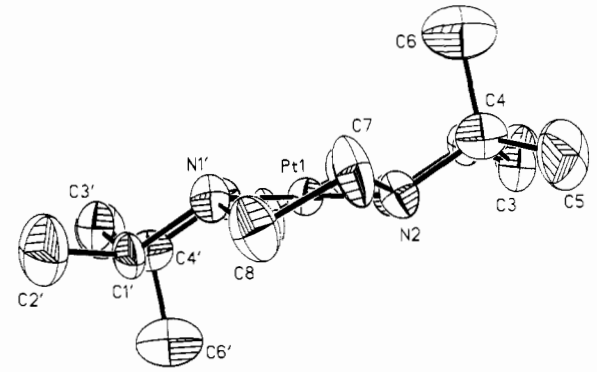

Figure 8. Side view of the macrocycle in $Pt(ms\text{-}(5,12)\text{-}Me_6[14]aneN_4)^{2+}$.

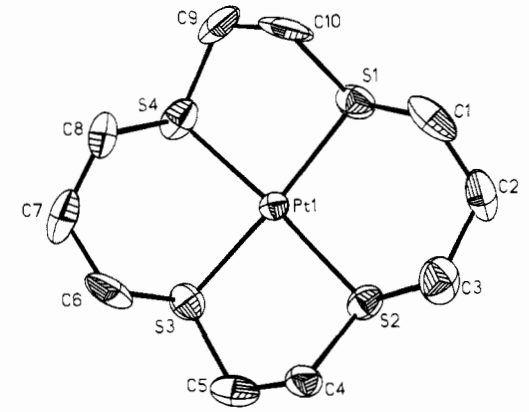

Figure 9. Perspective view of $Pt([14]aneS_4)^{2+}$.

crystallographic inversion center. The Pt and the four nitrogen atoms define a plane, and the displacements from this plane of the carbon atoms in the macrocyclic rings are listed in Table IX. The five-membered en rings are gauche $\delta\lambda$, and the six-membered rings assume the chair conformation. The configuration at the N atoms is meso-*RSSR*, type III.[34,35] Bite angles of the chelate rings are 85.0 (3)° for en and 95.0 (3)° for pn. Altogether, the geometry and conformation of the $Me_6[14]aneN_4$ ligand are entirely similar to those of $[14]aneN_4$ in the accompanying structure of $Pt([14]aneN_4)Cl_2^{2+}$. The cation is shown from a side perspective in Figure 8. The Pt–N length is normal at 2.05 (1) Å.

$[Pt([14]aneS_4)](ClO_4)_2$. Final fractional coordinates are given in Table VII. Labeling is shown in Figure 9. Bond lengths and angles are listed in Table VIII. The Pt environment is approximately square planar. The Pt atom occupies the four-sulfur donor plane (deviations +0.008, −0.012, +0.012, −0.013, +0.013 Å for Pt, S1, S2, S3, S4, respectively). The configuration at the S atoms is meso-*RSRS*, which has been designated type I (lone pairs up–up–up–up).[35,36] This configuration puts all ligand atoms below the four-sulfur donor plane. The ligand arrangement is illustrated

Table VII. Fractional Atomic Positional Parameters for $[Pt([14]aneS_4)](ClO_4)_2$

atom	x	y	z
Pt1	0.43202 (4)	0.08807 (4)	0.08036 (4)
S1	0.6146 (3)	0.0864 (4)	0.1567 (3)
S2	0.3889 (3)	−0.0770 (3)	0.1356 (3)
S3	0.2482 (3)	0.1024 (3)	0.0015 (3)
S4	0.4617 (3)	0.2547 (3)	0.0181 (3)
C1	0.630 (1)	0.022 (1)	0.288 (1)
C2	0.589 (1)	−0.091 (1)	0.278 (1)
C3	0.460 (1)	−0.102 (1)	0.269 (1)
C4	0.249 (1)	−0.050 (1)	0.162 (1)
C5	0.182 (1)	−0.008 (1)	0.056 (1)
C6	0.201 (1)	0.214 (1)	0.072 (1)
C7	0.249 (2)	0.315 (1)	0.043 (1)
C8	0.373 (1)	0.335 (1)	0.085 (1)
C9	0.601 (1)	0.288 (1)	0.085 (1)
C10	0.630 (1)	0.224 (1)	0.191 (1)
Cl1	−0.0411 (3)	0.0702 (3)	0.2638 (3)
O1	0.063 (1)	0.111 (1)	0.280 (2)
O2	−0.078 (1)	0.041 (1)	0.357 (1)
O3	−0.042 (1)	−0.022 (1)	0.206 (1)
O4	−0.111 (1)	0.147 (1)	0.212 (1)
Cl2	0.3780 (4)	0.1675 (3)	0.4177 (3)
O5	0.322 (1)	0.2362 (9)	0.473 (1)
O6	0.372 (1)	0.177 (1)	0.3108 (9)
O7	0.338 (2)	0.065 (1)	0.442 (2)
O8	0.482 (1)	0.160 (2)	0.464 (1)

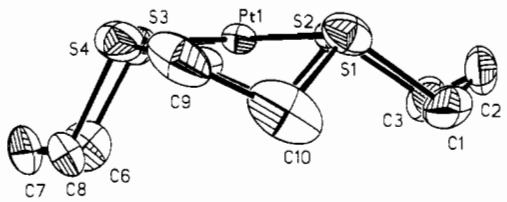

Figure 10. Side view of the macrocycle in $Pt([14]aneS_4)^{2+}$ illustrating the noncrystallographic mirror plane in the molecule.

in Figure 10, which also shows the noncrystallographic mirror plane present in the cation passing through atoms C2, Pt, and C7. The five-membered en chelate rings are very distorted from the usual gauche conformation but are chemically equivalent and have bite angles 87.3 (1) and 87.7 (1)°. The six-membered pn chelate rings however are decidedly inequivalent. Ring 1 containing S1, C1–C3, and S2 has a bite angle of 96.6 (1)° and less favorable torsion angles (S–C–C–C = 81 (1) and −80 (1)°; C–S–C–C = −160 (1) and 164 (1)°), assuming that the ideal geometry is represented by gauche (±60°) and anti (180°) arrangements. Ring 2 containing S3, C6–C8, and S4 has a smaller pn bite angle of 88.4 (1)° and less strained torsion angles (S–C–C–C = −71 (1) and 72 (1)°; C–S–C–C = 178 (1) and −177.5 (9)°). Both pn rings are in chair conformations. The closest approaching molecule to the free axial site of Pt is another cation related by an inversion center. Contact distances between the pair are Pt1···S1′ = 3.680 Å and Pt1···S2′ = 3.721 Å and are shown in Figure 11.

Discussion

There has been extensive use of macrocyclic ligands to explore the chemistry of transition metals, especially cobalt, nickel, and copper. Lots of structural information is available, most of it involving N, S, and O donor atoms in the macrocycle. The range of ring sizes concentrates on 14- and 16-membered rings because of the stability of ethylene and propylene 5- and 6-membered chelate linkages. Square planar (endo) geometry is the usual mode of bonding although exo-bridging modes and other geometries (e.g. square pyramidal) are not uncommon. In light of this and the early importance of square-planar Pt complexes to structural transition-metal chemistry, there are surprisingly few structural studies of Pt macrocyclic complexes. Those that have been characterized in the endo form include a $([16]aneN_2S_2)Pt^{II}$ complex,[25] an (N_4-tetrabenzo[16]annulene)Pt^{II} complex,[26] and an $([18]aneS_6)Pt^{II}$ complex.[27] The only reports of 14-membered

Table VIII. Bond Lengths (Å) and Angles (deg) for $[Pt([14]aneS_4)](ClO_4)_2$

Pt1–S1	2.271 (3)	C2–C3	1.55 (2)
Pt1–S2	2.285 (4)	C4–C5	1.55 (2)
Pt1–S3	2.301 (3)	C6–C7	1.47 (2)
Pt1–S4	2.295 (4)	C7–C8	1.53 (2)
S1–C1	1.83 (1)	C9–C10	1.55 (2)
S1–C10	1.80 (2)	Cl1–O1	1.35 (1)
S2–C3	1.79 (1)	Cl1–O2	1.37 (1)
S2–C4	1.81 (1)	Cl1–O3	1.38 (1)
S3–C5	1.80 (2)	Cl1–O4	1.38 (2)
S3–C6	1.81 (2)	Cl2–O5	1.35 (1)
S4–C8	1.78 (1)	Cl2–O6	1.34 (1)
S4–C9	1.81 (2)	Cl2–O7	1.43 (2)
C1–C2	1.51 (2)	Cl2–O8	1.31 (2)
Pt1–S1–C1	110.4 (5)	S4–C8–C7	111.8 (9)
Pt1–S1–C10	98.8 (5)	S4–C9–C10	111 (1)
Pt1–S2–C3	110.2 (5)	C1–S1–C10	102.9 (8)
Pt1–S2–C4	98.6 (4)	C1–C2–C3	114 (1)
Pt1–S3–C5	103.4 (5)	C3–S2–C4	101.0 (6)
PT1–S3–C6	102.1 (5)	C5–S3–C6	103.4 (7)
Pt1–S4–C8	103.0 (4)	C6–C7–C8	118 (1)
Pt1–S4–C9	103.7 (5)	C8–S4–C9	103.3 (7)
S1–Pt1–S2	96.6 (1)	O1–Cl1–O2	113 (1)
S1–Pt1–S3	176.0 (2)	O1–Cl1–O3	110 (1)
S1–Pt1–S4	87.7 (1)	O1–Cl1–O4	106.9 (9)
S1–C1–C2	110.8 (9)	O2–Cl1–O3	104.1 (8)
S1–C10–C9	107 (1)	O2–Cl1–O4	110.0 (9)
S2–Pt1–S3	87.3 (1)	O3–Cl1–O4	112.8 (9)
S2–Pt1–S4	175.7 (1)	O5–Cl2–O6	119.9 (9)
S2–C3–C2	112.4 (9)	O5–Cl2–O7	105.3 (9)
S2–C4–C5	106.5 (8)	O5–Cl2–O8	110 (1)
S3–Pt1–S4	88.4 (1)	O6–Cl2–O7	109 (1)
S3–C5–C4	113 (1)	O6–Cl2–O8	111 (1)
S3–C6–C7	113 (1)	O7–Cl2–O8	100 (1)

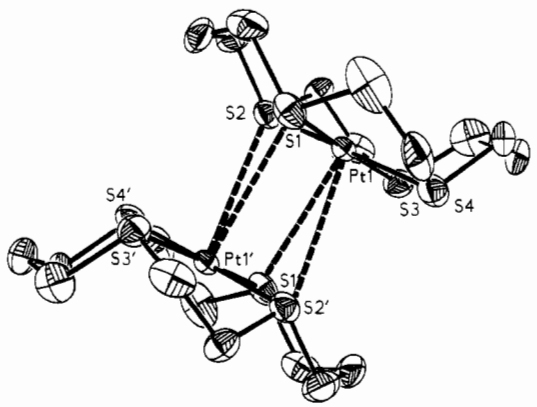

Figure 11. Two molecules of $Pt([14]aneS_4)^{2+}$ illustrating the intermolecular contact distances. Pt···S1′ = 3.680 Å, and Pt···S2′ = 3.721 Å.

macrocyclic complexes of Pt are for complexes with unsaturated ligands[28,29] and dioxocyclam.[24] It is therefore very appropriate to examine the structural characteristics of Pt with a series of 14-membered saturated ligands: $Pt([14]aneN_4)Cl_2^{2+}$, Pt(*ms*-(5,12)-Me_6[14]aneN$_4$)$^{2+}$, and $Pt([14]aneS_4)^{2+}$.

It is most common for [14]aneN$_4$ to bond to transition metals in either a planar (trans) type III configuration or a folded (cis) type V configuration.[37,38] The ligand configuration of [14]aneN$_4$ and *ms*-(5,12)-Me$_6$[14]aneN$_4$ reported here (planar, type III) with Pt is normal and is of lowest energy. There are several related discrete complexes that compare similarly, and these are listed in Table X. This table contains entries of wholly monodentate ligands, bidentate en and pn ligands, tetradentate [14]aneN$_4$ and derivative ligands, and one hexadentate cage complex. The little variation that is evidenced in Pt–N lengths can be easily accounted for by unsaturation in the ligand (i.e. dbtaa and dioxocyclam).

(37) Of the 32 hits in the Cambridge Structural Database[38] for transition-metal cyclam complexes, 24 are planar type III, 7 are folded type V, and 1 is planar type V.

(38) Allen, F. H.; Kennard, O.; Taylor, R. *Acc. Chem. Res.* **1983**, *16*, 146.

Table IX. Comparison of Ligand Conformations[a]

confign type	M–D, Å	D–M–D_{en}, deg	C dev from D_2M plane (en), Å	D–M–D_{pn}, deg	C dev from D_2M plane (pn), Å
			trans-$Pt^{IV}Cl_2([14]aneN_4)^{2+}$		
III	2.04 (1)	84.3 (5)	+0.36, −0.39	95.7 (5)	+0.86, +0.45, +0.81
			$Pt^{II}(Me_6[14]aneN_4)^{2+}$		
III	2.05 (1)	85.0 (3)	+0.42, −0.33	95.0 (3)	+0.83, +0.39, +0.80
			$Pt^{II}([14]aneS_4)^{2+}$		
I	2.29 (1)	87.3 (1)	+1.05, +0.37	88.4 (1)	+1.57, +1.53, +1.54
		87.7 (1)	+0.28, +1.01	96.6 (1)	+1.09, +0.60, +1.03
			$Pd^{II}([14]aneS_4)^{2+}$		
I	2.27 (2)	89.6	+1.03, +0.21	88.2	+1.54, +1.65, +1.71
		87.0	+0.40, +0.95	95.1	+1.26, +0.79, +1.01

[a] S or N donor atoms in the macrocycle are designated D in the table headings. Data for $Pd([14]aneS_4)^{2+}$ were taken from ref 49; other data are from this work.

Table X. Structural Comparisons of Pt/Pd Tetraamine Complexes

complex	M–N, Å	M–Cl, Å	N–M–N_{en} bite angle, deg	N–M–N_{pn} bite, angle, deg	ref
		M(IV) Complexes			
trans-$Pt(NH_3)_4Cl_2^{2+}$	2.054 (5)	2.306 (5)			*a*
trans-$Pt(en)_2Cl_2^{2+}$	2.081 (8)	2.313 (4)	82.7 (5)		*b*
trans-$Pt(pn)_2Cl_2^{2+}$	2.069 (4)	2.304 (1)		94.1 (2)	*c*
trans-$Pt(dbtaa)I_2^{2+}$	1.99 (2)		81 (1)	99 (1)	*d*
trans-$PtCl_2([4]aneN_4)^{2+}$	2.04 (1)	2.307 (4)	84.3 (5)	95.7 (5)	*e*
$Pt((NHOH)_2sar)^{2+}$	2.06 (2)		85 (1)	91 (3)	*f*
trans-$Pd([14]aneN_4)^{2+}$	2.062 (4)	2.303 (1)	84.7 (1)	95.3 (1)	*g*
		M(II) Complexes			
$Pt(NH_3)_4^{2+}$	2.055 (4)				*h*
$Pt(en)_2^{2+}$	2.037 (9)		83.3 (6)		*i*
$Pt(pn)_2^{2+}$	2.055 (5)			91.3 (1.3)	*j*
$Pt(dbtaa)^{2+}$	1.98 (2)		83 (3)	96 (3)	*d*
$Pt(dioxocyclam)^{2+}$	2.06 (1)[k]		83.9 (7)	97.1 (4)[k]	*l*
	1.98 (1)[m]			95.2 (5)[m]	
$Pt(ms\text{-}(5,12)\text{-}Me_2[14]aneN_4)^{2+}$	2.05 (1)		85.0 (3)	95.0 (3)	*e*
$Pd([14]aneN_4)^{2+}$	2.051 (7)		83.0 (3)	97.1 (1.0)	*g*

[a] Balde, L.; Khodadad, P.; Rodier, N. *Acta Crystallogr.* **1989**, *C45*, 859. [b] Larsen, K. P.; Hazell, R. G.; Toftlund, H.; Andersen, P. R.; Bisgard, P.; Edlund, K.; Eliasen, M.; Herskind, C.; Laursen, T.; Pedersen, P. M. *Acta Chem. Scand.* **1975**, *A29*, 499. [c] Delafontaine, J.-M.; Toffoli, P.; Khodadad, P.; Rodier, N. *Acta Crystallogr.* **1988**, *C44*, 66. [d] Reference 29. [e] This work. [f] Hagen, K. S.; Lay, P. A.; Sargeson, A. M. *Inorg. Chem.* **1988**, *27*, 3424. [g] Reference 23. [h] Rochen, F. D.; Melanson, R. *Acta Crystallogr.* **1980**, *B36*, 691. Khodadad, P.; Rodier, N. *Acta Crystallogr.* **1987**, *C43*, 1690. [i] Freeman, W. A. *Inorg. Chem.* **1976**, *15*, 2235–2239. Robinson, P. R.; Schlemper, E. O.; Murmann, R. K. *Inorg. Chem.* **1975**, *14*, 2035. [j] Viossat, B.; Toffoli, P.; Khodadad P.; Rodier, N. *Acta Crystallogr.* **1987**, *C43*, 855. [k] These values were averaged by using only the saturated end of the ligand. [l] Reference 24. [m] These values were averaged by using only the unsaturated end of the ligand.

There is no significant difference in Pt(II)–N and Pt(IV)–N distances, and the ionic radii[39] of Pt(II) (0.74 Å for 4-coordinate square planar) and Pt(IV) (0.77 Å for 6-coordinate) are nearly equivalent. The complexes of cyclam with Pd(II) and Pd(IV) are known, and they are included in Table X, since their geometries are practically identical with those of the Pt compounds listed.

The ligand $[14]aneS_4$, like $[14]aneN_4$, has been widely studied in transition-metal coordination chemistry.[14] It too possesses both an exo conformation, where the metal binds externally to the macrocyclic cavity,[40-44] and an endo conformation, wherein the metal resides within the cavity. In the endo conformation, $[14]aneS_4$ has been seen to bind one metal in a planar S environment of type III configuration with the first-row transition metals Cu(II)[45,46] and Ni(II).[47] In a type III configuration, the carbon backbone atoms of the ligand are distributed to either side of the MS_4 plane. Structural studies on the larger ions with $[14]aneS_4$ have shown a preference for the type I configuration in either a planar trans arrangement (M = Rh(I),[48] Pd(II),[49] Hg(II)[41]) or the folded cis arrangement (M = Ru(II),[50] Ir(III)[51]). In the planar geometry, the type I configuration requires all ligand atoms to occupy one side of the MS_4 plane, as shown for $Pt([14]aneS_4)^{2+}$ in Figure 10. This configuration has been associated with increased nucleophilicity in the Rh(I) complexes, since the open face provides better access in solution.[48] In the crystalline form of $Pt([14]aneS_4)^{2+}$, the open coordination face is associated with another molecule to form loose dimers (see Figure 11). The $Rh([14]aneS_4)^+$ complex also dimerizes in this manner and Rh···S bonding interactions have been postulated because Rh···S = 3.70–3.82 Å and the Rh is displaced from the four-sulfur plane by 0.133 Å toward the intermolecular S atom. For the complex

(39) Ionic radii quoted were taken from the compilation given in: Huheey, J. E. *Inorganic Chemistry*, 3rd ed.; Harper & Row: New York, 1983; p 73.
(40) DeSimone, R. E.; Glick, M. D. *J. Coord. Chem.* **1976**, *5*, 181.
(41) Alcock, N. W.; Herron, N.; Moore, P. *J. Chem. Soc., Dalton Trans.* **1978**, 394.
(42) Galesic, N.; Herceg, M.; Sevdic, D. *Acta Crystallogr.* **1986**, *C42*, 565.
(43) Diaddario, L. L.; Dockal, E. R.; Glick, M. D.; Ochrymowycz, L. A.; Rorabacher, D. B. *Inorg. Chem.* **1985**, *24*, 356.
(44) Robinson, G. H.; Zhang, H.; Atwood, J. L. *Organometallics* **1987**, *6*, 887.
(45) Glick, M. D.; Gavel, D. P.; Diaddario, L. L.; Rorabacher, D. B. *Inorg. Chem.* **1976**, *15*, 1190.
(46) The energy differences between the type I and III configurations of [14]aneS$_4$ complexes may be relatively small: Desper, J. M.; Gellman, S. H. *J. Am. Chem. Soc.* **1991**, *113*, 704.
(47) Davis, P. H.; White, L. K.; Belford, R. L. *Inorg. Chem.* **1975**, *4*, 1753.
(48) Yoshida, T.; Ueda, T.; Adachi, T.; Yamamoto, K.; Higuchi, T. *J. Chem. Soc., Chem. Commun.* **1985**, 1137.
(49) Bell, M. N.; Blake, A. J.; Gould, R. O.; Holder, A. J.; Hyde, T. I.; Lavery, A. J.; Reid, G.; Schröder, M. *J. Inclusion Phenom.* **1987**, *5*, 169.
(50) Lai, T.-F.; Poon, C.-K. *J. Chem. Soc., Dalton Trans.* **1982**, 1465.
(51) Blake, A. J.; Gould, R. O.; Reid, G.; Schroder, M. *J. Organomet. Chem.* **1988**, *356*, 389–396.

Scheme I

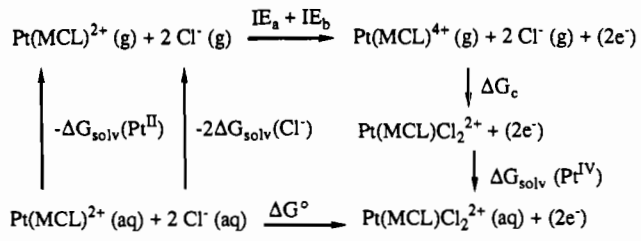

reported here, Pt([14]aneS$_4$)$^{2+}$, definite bonding interactions between intermolecular Pt and S are less likely: Pt···S1′ = 3.68 Å and Pt···S2′ = 3.72 Å [note that Pt(II) is a smaller ion than Rh(I)]; the Pt is occupying the four-sulfur plane, and the Pt···S′ contact is not in a direct axial position. The vector Pt–S1′ makes an angle of 63.6 (4)° with the four-sulfur macrocyclic plane, and the Pt–S2′ vector is at 61.6 (3)° to this four-sulfur plane.

The Pt–S bond length in Pt([14]aneS$_4$)$^{2+}$ (2.29 (1) Å) compares favorably with that of the square-planar 4-coordinate complexes Pt([18]aneS$_6$)$^{2+}$ (2.296 Å), Pd([18]aneS$_6$)$^{2+}$ (2.309 Å), and Pd([14]aneS$_4$)$^{2+}$ (2.25–2.30 Å).[51] The distortions in the chelate rings of the type I complexes Pt([14]aneS$_4$)$^{2+}$ and Pd([14]aneS$_4$)$^{2+}$ are entirely similar and can be seen in the carbon atom displacements in Table IX, which also contrasts them with the more normal (lower energy) configurations of the macrocyclic in Pt([14]aneN$_4$)Cl$_2^{+}$ and Pt([14]aneN$_4$)$^{2+}$.

Oxidation–Reduction Chemistry of the Complexes. The trends in electrochemical behavior of these complexes are likely to reflect variations in both the stereochemical properties of the ligands and the electronic coupling between the ligand and the metal. The quasi-reversible oxidations of Pt(MCL)$^{2+}$ (where MCL = a macrocyclic ligand) in 1 M aqueous NaCl solutions are in most cases associated with the Pt(IV)–Pt(II) couple, and there are only a few systems in which the electrochemical behavior might be construed to indicate that the intermediate Pt(MCL)$^{3+}$ complex persists long enough to strongly perturb the electrochemistry (at least in the 1 M NaCl solutions). Consequently, we interpret the prevailing electrochemical behavior as

$$Pt(MCL)^{2+} + 2Cl^- \overset{K_1}{\rightleftharpoons} \{Pt(MCL)^{2+},2Cl^-\} \quad (1)$$

$$\{Pt(MCL)^{2+},2Cl^-\} \rightleftharpoons \{Pt(MCL)Cl_2^{+}\} + e^- \quad (2)$$

$$\{Pt(MCL)Cl_2^{+}\} \rightleftharpoons Pt(MCL)Cl_2^{2+} + e^- \quad (3)$$

where the {Pt(MCL)$^{2+}$,2Cl$^-$} species is presumed to be an ion pair and {Pt(MCL)Cl$_2^{+}$} is a transient intermediate oxidized more easily than its precursor. Thus, the net electrochemical reaction becomes

$$\{Pt(MCL)^{2+},2Cl^-\} \rightleftharpoons Pt(MCL)Cl_2^{2+} + 2e^- \quad (4)$$

The factors affecting this reaction are conveniently discussed in terms of eqs 1 and 5. Since their charge types and external

$$\{Pt(MCL)^{2+},2Cl^-\} \rightleftharpoons Pt(MCL)Cl_2^{2+} + 2e^- \quad (5)$$

dimensions do not vary a great deal, most of the Pt([n]aneN$_a$S$_b$)$^{2+}$ complexes (n = 13–16; a + b = 4) probably have comparable values of K_1, and their variations in $E_{1/2}$ values must arise from eq 5. In order to approach the factors that contribute to variations in this quantity, it is useful to reformulate the oxidation process in terms of the simple free energy cycle presented in Scheme I. For this cycle

$$-nFE^\circ = \Delta G^\circ = \Delta(\Delta G_{solv}) + IE_a + IE_b + \Delta G_c \quad (6)$$

Variations in $\Delta(\Delta G_{solv})$ are probably small so that we can interpret the larger contributions of "electronic" factors in terms of contributions of the ionization energy terms (IE_a + IE_b), and the stereochemical contributions will predominantly occur as variations in ΔG_c. Of course, there can be important stereochemical contributions to ΔG_{solv}(Pt^{II} or Pt^{IV}), and electronic factors might make small contributions to ΔG_c (these amount to variations in the contributions of off-diagonal terms in the energy matrix).

Stereochemical factors are clearly very important. Thus, the Me$_6$[14]aneN$_4$ ligands differ from [14]aneN$_4$ only in the methyl substitution at the periphery of the molecule. The 0.2 V greater half-wave potential for the oxidation of the Pt(Me$_6$[14]aneN$_4$)$^{2+}$ complexes than for their Pt([14]aneN$_4$)$^{2+}$ analogues is most likely a stereochemical effect related to the coordination of two axial ligands to Pt(IV) (thus a contribution to ΔG_c) and is typical of this group of ligands.[52]

Electronic effects related to hole size have often been discussed for complexes of the [n]aneN$_4$ ligands.[3-5,31] For example, the M^{III,II}([15]aneN$_4$) couples are significantly (typically 0.2–0.3 V) more oxidizing than the M^{III,II}([14]aneN$_4$) couples of the M = Co[53] and Ni[52] complexes. That the Pt^{IV,II}([15]aneN$_4$) and Pt^{IV,II}([14]aneN$_4$) couples have very similar values of $E_{1/2}$ suggests that the changes in equatorial coordination affect both platinum oxidation states to the same degree. In contrast, we have found a strong apparent trend of decreasing values of $E_{1/2}$ with increasing [n]aneS$_4$ ring size for the Pt(IV)/Pt(II) couples. At least part of this variation is probably stereochemical. The X-ray structure shows that the [14]ane S$_4$ ligand has assumed the type I configuration in Pt([14]aneS$_4$)$^{2+}$, in which it is folded away from one side of the molecule, somewhat restricting approach to axial coordination site on the opposite side of the molecule. This is likely to slightly destabilize the Pt(IV) complex (i.e., through ΔG_c), resulting in a relatively positive potential.[54] Increases in ring size most likely reduce these stereochemical stresses, hence the decreases in $E_{1/2}$. A very similar situation has been found for Cu([n]aneS$_4$)$^{2+}$ complexes in which the Cu([12]aneS$_4$)$^{2+}$ and the Cu([13]aneS$_4$)$^{2+}$ complexes have the folded conformation analogous to that found for Pt([14]aneS$_4$)$^{2+}$, while Cu(II) complexes with larger rings (n = 14–16) have a ligand conformation with the metal more nearly centered in the ring.[31] An increase of the Cu(II)/Cu(I) potentials with increasing MCL ring size has also been observed ($E_{1/2}$ = 0.52–0.71 V for n = 13–16, respectively),[55] but the stereochemical changes are more complex in the Cu(II)/Cu(I) than in the Pt(IV)/Pt(II) systems (approximately $D_{4h} \rightarrow T_d$ compared to $D_{4h} \rightarrow D_{4h}$, respectively).

There is also a systematic increase of $E_{1/2}$ as N is replaced by S in [14]aneN$_a$S$_b$ complexes (Figure 4). The range of $E_{1/2}$ values found on replacing N$_4$ by S$_4$ donors (0.46 V) is about twice the ranges of potentials induced by the stereochemical perturbations noted above (0.16 V for ring sizes of S$_4$ donors; 0.22 V for [14]aneN$_4$ compared to Me$_6$[14]aneN$_4$). Much of this variation in $E_{1/2}$ values must also be stereochemical, since the more symmetric, type III, ligand configuration is found for Pt([14]aneN$_4$)Cl$_2^{2+}$ and Pt(*ms*-(5,12)-Me$_6$[14]aneN$_4$)$^{2+}$. These stereochemical contrasts probably originate in the smaller size of N compared to S, so that the values of $E_{1/2}$ again increase as stereochemical congestion of the axial coordination sites increases.

There is also some possibility that some of the shift in potential of Pt(IV)/Pt(II) couples that accompanies the substitution of an S donor for an N donor ligand could be the result of an electronic contribution (such as might be ascribed to variations in the "hard–soft" donor–acceptor interactions). Our observations suggest that such electronic factors contribute less than 0.06 V per donor–acceptor bond to the variations in Pt(IV)/Pt(II) potentials. Since the stereochemical perturbations that we have employed do not directly reflect on the net stereochemical consequences of the larger C–N–C compared to C–S–C bond angles, the actual electronic influence on the Pt(IV)/Pt(II) potentials may be significantly less than the very crude estimate above. Once again, it is important to recall that the values of $E_{1/2}$ are only altered by factors which differ for Pt(IV) and Pt(II) and that the most striking difference is the contrast in coordination numbers.

(52) Busch, D. H.; Pillsbury, D. G.; Lovechio, F. V.; Tait, A. M.; Hung, Y.; Jackels, S.; Rabowski, M. C.; Schammel, W. D.; Martin, L. Y. In *Electrochemical Studies of Biological Systems*; Sawyer, D. T., Ed.; ACS Symposim Series 38; American Chemical Society: Washington, DC, 1977; p 32.
(53) Endicott, J. F.; Durham, B.; Kumar, K. *Inorg. Chem.* **1982**, *21*, 2437.
(54) Note that the maximum range of variation in ΔG_c would be about 40 kJ mol^{-1} (or 20 kJ mol^{-1} per axial bond).
(55) Bernardo, M. M.; Schroeder, R. R.; Rorabacher, D. B. *Inorg. Chem.* **1991**, *30*, 1241.

Conclusions

By employing relatively small variations in the size and substituents of macrocyclic, equatorial ligands, we have shown that stereochemical influences result in substantial alterations of the Pt(IV)/Pt(II) reduction potential and that these influences correlate with inhibitions of axial binding in the Pt(IV) complex. These observations suggest that related stereochemical alterations could be used to decrease the tendency of metastable Pt(III) species to disproportionate, since axial bonding is expected to be relatively weak in the low-spin d^7 electronic configuration.

Acknowledgment. The diffractometer used herein was purchased by an NSF equipment grant to Wayne State University. The Cambridge Structural Database[38] assisted in the literature searches. We are grateful to Professor D. B. Rorabacher for useful discussions, for providing access to some of the ligands, and for providing us with the report of some of his unpublished work. We also thank Mr. Michael J. Mayer for help with ligand syntheses.

Supplementary Material Available: Tables A and B, giving thermal parameters and hydrogen atomic positions for [*trans*-Pt([14]aneN$_4$)Cl$_2$]Cl$_2$·HCl·H$_2$O, Tables D and E, giving thermal parameters and hydrogen atomic positions for [Pt(*ms*-(5,12)-Me$_6$[14]aneN$_4$)](ClO$_4$)$_2$·2H$_2$O, and Tables G and H, giving thermal parameters and hydrogen atomic positions for [Pt([14]aneS$_4$)](ClO$_4$)$_2$ (5 pages); Tables C, F, and I, listing observed and calculated structure factors for the three complexes (47 pages). Ordering information is given on any current masthead page.

Contribution from the Department of Chemistry, Gorlaeus Laboratories, Leiden University, P.O. Box 9502, 2300 RA Leiden, The Netherlands

Nickel Template Syntheses of Pentadentate and Macrocyclic Nitrogen–Sulfur Ligands: Single-Crystal X-ray Structure of (1,10-Diaza-4,7,13,16-tetrathia-5,6:14,15-dibenzocyclooctadecane)nickel(II) Bis(tetraphenylborate)–Acetonitrile(1/3)

Nadine de Vries and Jan Reedijk*

Received February 5, 1991

Complexes of nickel with macrocyclic and pentadentate nitrogen–sulfur donor ligands have been prepared via the reaction of [Ni(bdt)$_2$]$^-$ with bis(2-chloroethyl)amine and 2,6-bis(chloromethyl)pyridine, respectively. The coordination sphere of the pentacoordinate compound (2,6-bis(((2-mercaptophenyl)thio)methyl)pyridinato)nickel(II) (**2**) consists of an aromatic amine, two thioether, and two thiolate donors. It is thermochromic, being yellow-orange at low temperatures and red-violet upon heating, and there is no major change in the vis-near-IR spectrum, which simply show a shift of λ_{max} from 480 to 520 nm. Magnetic measurements indicate that the compound contains high-spin Ni(II) (μ_{eff} 3.05 μ_B). A rather low quasi-reversible oxidation potential is observed at +0.144 V (all potentials are reported vs SCE), a second is observed at +0.546 V, and two irreversible reduction potentials are observed at −0.754 and −1.228 V. The hexadentate, macrocyclic complex (1,10-diaza-4,7,13,16-tetrathia-5,6:14,15-dibenzocyclooctadecane)nickel(II) bis(tetraphenylborate) (**3**) was characterized by X-ray crystallography, which showed the complex to be a distorted octahedron with the four thioether donors (Ni–S = 2.398 (2), 2.440 (2) Å) in the equatorial plane and the nitrogen atoms (Ni–N = 2.082 (4) Å) in the axial positions. Crystal data are a = 18.213 (4) Å, b = 18.213 (12) Å, c = 20.115 (8) Å, and β = 103.51° with space group $C2/c$, Z = 4, R = 0.0434, and R_w = 0.0434. This complex has a high, irreversible oxidation potential at +0.964 V and a quasi-reversible reduction wave at −0.864 V. No hydrogen bonding is observed in the solid state but the N–H stretch of the amine is lowered to 3200 cm^{-1} upon coordination to the nickel ion.

Since the relatively recent discovery that a number of hydrogenases contain nickel, many studies have been carried out[1,2] in attempts to elucidate the role of nickel in catalyzing the reaction $H_2 \rightleftharpoons 2H^+ + 2e^-$. The EPR spectrum of these enzymes changes upon exposure to molecular hydrogen, giving rise to signals that can be attributed to Ni(I).[3-5] ESEEM evidence suggests that there is nitrogen in the coordination sphere,[6] and EXAFS studies indicate that sulfurs (probably three or four) are the predominant donors.[7,8] The salient feature of these nickel centers are the very low Ni(II)/Ni(III) oxidation potentials of −0.390 to −0.640 V (vs SCE),[1,9,10] which is striking when compared to the values reported for classical coordination compounds of nickel (+0.50 to +1.50 vs SCE).[11-13] An exception is [Ni(S$_2$-norbornane)$_2$]$^{2-}$, reported by Millar, which contains nickel coordinated by four thiolates and has an oxidation potential at −0.76 V (vs SCE).[14] Since no hydrogenase has yet been subjected to an X-ray crystallographic structure determination, there is still considerable speculation as to the nature of the nickel site.

Recently a number of model compounds have been synthesized in hopes of mimicking the properties of the nickel site in hydrogenases.[15-21] In search for complexes of nickel with novel

(1) Walsh, C. T.; Orme-Johnson, W. H. *Biochemistry* **1987**, *26*, 4901.
(2) Hausinger, R. P. *Microbiol. Rev.* **1987**, *51*, 22.
(3) Coremans, J. M. C. C.; Van der Swaan, J. W.; Albracht, S. P. J. *Biochim. Biophys. Acta* **1989**, *997*, 256.
(4) Van der Zwaan, J. W.; Albracht, S. P. J.; Fontijn, R. D.; Mul, P. *Eur. J. Biochem.* **1987**, *169*, 377.
(5) Teixeira, M.; Moura, I.; Xavier, A. V.; Huynh, B. H.; DerVartanian, D. V.; Peck, H. D., Jr.; LeGall, J.; Moura, J. J. G. *J. Biol. Chem.* **1985**, *260*, 8942.
(6) Chapman, A.; Commack, R.; Hatchikian, C. E.; McCracken, J.; Peisach, J. *FEBS Lett.* **1988**, *242*, 134.
(7) Lindahl, P. A.; Kojima, N.; Hausinger, R. P.; Fox, J. A.; Teo, Boon, K.; Walsh, C. T.; Orme-Johnson, W. H. *J. Am. Chem. Soc.* **1984**, *106*, 3062.
(8) Scott, R. A.; Wallin, S. A.; Czechowski, M.; DerVartanian, D. V.; LeGall, J.; Peck, H. D., Jr.; Moura, I. *J. Am. Chem. Soc.* **1984**, *106*, 6864.
(9) *The Biochemistry of Nickel*; Lancaster, J. R., Jr., Ed.; VCH Publishers, Inc.: New York, 1988.
(10) Cammack, R. *Adv. Inorg. Chem.* **1988**, *32*, 297.
(11) Nag, K.; Chakravorty, A. *Coord. Chem. Rev.* **1980**, *33*, 87.
(12) Haines, R. I.; McAuley, A. *Coord. Chem. Rev.* **1981**, *39*, 77.
(13) Lappin, A.; McAuley, A. *Adv. Inorg. Chem.* **1988**, *32*, 241.
(14) Fox, S.; Yun, W.; Silver, A.; Millar, M. *J. Am. Chem. Soc.* **1990**, *112*, 3218.
(15) Rosenfield, S. G.; Wong, M. L. Y.; Stephan, D. W.; Mascharak, P. K. *Inorg. Chem.* **1987**, *26*, 4119.
(16) Baidya, N.; Olmstead, M. M.; Mascharak, P. K. *Inorg. Chem.* **1989**, *28*, 3426.
(17) Rosenfield, S. G.; Berends, H. P.; Gelmini, L.; Stephan, D. W.; Mascharak, P. K. *Inorg. Chem.* **1987**, *26*, 2792.
(18) Blake, A. J.; Lavery, A. J.; Hyde, T. I.; Schröder, M. *J. Chem. Soc., Dalton Trans.* **1989**, 965.

0020-1669/91/1330-3700$02.50/0